region of the left flank of the curve where, according to theory, the Compton component will not yet have developed an important intensity. The existence of a region free of Compton scattering can be investigated by calculating the ratio of the ordinates of Figs. 4 and 5 after subtracting the continuous backgrounds. We found by this method that, in effect, the ratio was constant on a considerable region of the left flank. By using this constant value as a scale factor, Figs. 4 and 5 can be plotted together (Fig. 6). They show good fit on the left side of the picture and a Compton component on the right. On Fig. 7 the two components have been drawn separately. The Compton spectrum shows a rather well-defined limit on the side of the short wavelengths. Figures 8, 9, and 10 represent the corresponding results for metallic lithium. We notice that, also in this case, the Compton component shows a well-defined limit (Fig. 10), but it is shifted towards shorter wavelengths than in Fig. 7 by 0.065°. The difference between the two limits gives an energy gap of 5.4 eV. The error is evaluated to ±0.8 eV. The curves of the Compton component in Figs. 7 and 10 cannot be compared directly with any theoretical curve of the Compton spectrum because, as mentioned, they are distorted. We notice that their general forms are similar but their widths differ by 15%. As the distorting effects are the same in both cases, we conclude that the Compton profile of LiD is wider than that of Li.

The effects of distortion can be evaluated in an approximate way, by the method proposed by Lord Rayleigh.[14] The deconvolution will give a sharper cutoff, a steeper and more rectilinear flank on the left side, a sharper maximum and minor changes of the form on the right side. The general form, however, will not change much.

[14] J. W. Strutt, 3rd Baron Rayleigh, *Scientific Papers* (Cambridge University Press, New York, 1899), Vol. I, p. 135.

PHYSICAL REVIEW VOLUME 140, NUMBER 2A 18 OCTOBER 1965

Shapes of Impurity Absorption Bands in Solids*†

THOMAS H. KEIL‡§
Institute of Optics, University of Rochester, Rochester, New York
(Received 27 May 1965)

Optical-absorption line shapes arising from interaction of the electronic states of impurities with the vibrational modes of the crystal are considered. It is shown that this line shape may be expressed as an N-fold convolution integral, where each element of the convolution is the line shape due to a single vibrational mode of the ground state of the system. Two types of vibrational modes, linear and quadratic, are considered in detail in both the semiclassical approximation and quantum mechanically. It is shown that the semiclassical approximation, although often of use for linear interactions, has limited validity for quadratic modes. Formal methods are developed for performing the convolution integral to obtain the line shape due to a number of vibrational modes. Explicit numerical examples are presented.

I. INTRODUCTION

PREVIOUS work on the influence of lattice vibrations on impurity absorption bands has centered largely on the simplest possible model of the lattice-impurity interaction, i.e., a linear interaction. Such a model was first considered by Muto,[1] Huang and Rhys,[2] and Pekar.[3] Their calculations were extended and formalized in an elegant paper by Lax[4] and later by O'Rourke.[5] This model has been successful in explaining the general features of the absorption line shape for several impurity centers.

For many impurity centers of interest, this simple model will not be wholly adequate. In particular, if the impurity site is a center of inversion, the linear interaction will vanish by symmetry for half of the vibrational modes (those of odd parity); and, for these modes, a quadratic interaction will dominate. Previously, such modes have been considered only in the so-called semiclassical approximation or in perturbation theory. In this work, the first thorough quantum treatment of line shapes due to quadratic modes is presented. The complications of quadratic modes are such that the

* Work supported in part by the National Science Foundation.
† Based in part on a thesis submitted to the University of Rochester in partial fulfillment of the requirements for the Ph.D. degree.
‡ National Science Foundation pre-doctoral fellow, 1964–65.
§ Present address: Solid State and Materials Programme, Princeton University, Princeton, New Jersey.
[1] T. Muto, Progr. Theoret. Phys. (Kyoto) 4, 181 (1949).
[2] K. Huang and A. Rhys, Proc. Roy. Soc. (London) A204, 406 (1950).
[3] S. Pekar, Zh. Eksperim. i Teor. Fiz. 20, 510 (1950); Uspekhi Fiz. Nauk 50, 193 (1953).
[4] M. Lax, J. Chem. Phys. 20, 1752 (1952).
[5] R. C. O'Rourke, Phys. Rev. 91, 265 (1953).

use of a digital computer in calculating the line shape is convenient.

In addition to the quantum theory of linear and quadratic modes, a commonly used method for determining the approximate line shape, the semiclassical approximation,[4] is considered. The limitations and range of validity of this method are carefully explored. In particular, it is found that the semiclassical approximation, although often useful for linear interactions, has extremely limited validity when applied to quadratic modes; and, in fact, often leads to completely erroneous results.

Contemporary with the work of Refs. 1 to 3, Williams,[6] and Williams and Hebb[7] independently developed another treatment. They considered a model, first proposed by von Hippel[8] and Seitz,[9] in which only one normal coordinate, referred to as the CC (configuration coordinate), interacts appreciably with the center. For many impurity centers, a single interaction is not an adequate description of the system, and any realistic model must include a variety of interacting modes. McCumber[10] has developed interesting formal methods for calculating the line shape when the interacting modes form a dense set. These methods are appropriate when the impurity has a relatively weak interaction with the host crystal, and have proved successful in fitting a number of experimentally observed line shapes. In this work, methods for including the interaction of an arbitrary number of vibrational modes, both linear and quadratic, are developed. These methods are particularly appropriate to a relatively tightly bound, strongly interacting impurity center.

The general plan of this work is as follows. In Sec. II the theory of absorption line shapes is considered in general terms. The principal result of this section is that the total line shape for an impurity center can be expressed as an N-fold convolution, where each element of the convolution is simply the line shape due to a single normal mode of the *ground state* of the system. The normal modes may then be divided into three types. The first type, the linear mode, is reviewed both quantum mechanically and in the semiclassical approximation in Sec. III.

Section IV is an exhaustive treatment of the second type of mode, the quadratic mode. The quantum theory of quadratic modes, first at zero temperature and then for finite temperatures, is considered. The final part of Sec. IV is a careful consideration of the semiclassical approximation as applied to quadratic modes, and its relation to the quantum theory. The third type of mode, which contains both linear and quadratic interactions, will not be considered here. Although modes of the third type present no new difficulties, the increase in algebraic complexity does not seem to be balanced by new physical insight.

In Sec. V, the formal methods necessary to perform the convolutions to obtain the line shape due to an arbitrary number of interacting modes are developed.

II. GENERAL THEORY OF ABSORPTION LINE SHAPES

A. The Line Shape Function

Following Lax[4] we can, in the adiabatic and Condon approximations, write the normalized line shape function, for transitions from electronic state a to electronic state b, as

$$I_{ab}(E)=\mathrm{Av}_\alpha \sum_\beta |\langle a\alpha|b\beta\rangle|^2 \delta(\epsilon_{b\beta}-\epsilon_{a\alpha}-E). \quad (2.1)$$

$\langle a\alpha|$ and $\langle b\beta|$ are the vibrational wave functions for the ground and excited electronic states, respectively, and satisfy

$$[T_N+E_i(\mathbf{X})]\psi_{i\gamma}(\mathbf{X})=\epsilon_{i\gamma}\psi_{i\gamma}(\mathbf{X}), \quad (2.2)$$

where $i\gamma$ stands for either $a\alpha$ or $b\beta$, T_N is the nuclear kinetic-energy operator, and $\mathbf{X}$ represents the nuclear coordinates. $E_i(\mathbf{X})$ is the adiabatic potential in which the nuclei move and is the energy eigenvalue of the electronic part of the adiabatic Hamiltonian[11] for state i,

$$[T_E+U(\mathbf{r},\mathbf{X})]\phi_i(\mathbf{r},\mathbf{X})=E_i(\mathbf{X})\phi_i(\mathbf{r},\mathbf{X}), \quad (2.3)$$

where T_E is the electronic kinetic-energy operator, $\mathbf{r}$ represents the electronic coordinates, and $U(\mathbf{r},\mathbf{X})$ stands for all the terms in the total Hamiltonian except the nuclear and electronic kinetic energies. Av_α stands for a thermal average over initial vibrational states and $\sum_\beta$ for a sum over final vibrational states.

The adiabatic potential $E_a(\mathbf{X})$ for the ground state may be expanded in a Taylor series in the displacements of the nuclei from their equilibrium positions. Performing a normal-mode transformation, the adiabatic potential becomes

$$E_a(\mathbf{X})=\sum_i \tfrac{1}{2}M_i\omega_{ia}^2Q_i^2, \quad (2.4)$$

where Q_i, M_i, and ω_{ia} are the normal coordinate, mass, and frequency of the ith normal mode. Using $T_N=-\sum_i(\hbar^2/2M_i)(\partial^2/\partial Q_i^2)$, Eq. (2.2) for the ground state may be written

$$\sum_i\left[-\frac{\hbar^2}{2M_i}\frac{\partial^2}{\partial Q_i^2}+\tfrac{1}{2}M_i\omega_{ia}^2Q_i^2\right]\psi_{a\alpha}(\mathbf{X})=E_{a\alpha}\psi_{a\alpha}(\mathbf{X}). \quad (2.5)$$

[6] F. E. Williams, J. Chem. Phys. **19**, 457 (1951).
[7] F. E. Williams and M. H. Hebb, Phys. Rev. **84**, 1181 (1951).
[8] A. von Hippel, Z. Physik **101**, 680 (1936).
[9] F. Seitz, Trans. Faraday Soc. **35**, 79 (1939).
[10] D. E. McCumber, Phys. Rev. **135**, A1676 (1964); J. Math. Phys. **5**, 221 (1964); **5**, 508 (1964).
[11] M. Born and K. Huang, *Dynamical Theory of Crystal Lattices* (Clarendon Press, Oxford, England, 1954), p. 406.

The solutions to Eq. (2.5) are

$$\psi_{a\alpha}(\mathbf{X})=\prod_i \varphi_{a\alpha_i}(Q_i), \tag{2.6}$$

where $\varphi_{a\alpha_i}(Q_i)$ satisfies

$$\left[-\frac{\hbar^2}{2M_i}\frac{\partial^2}{\partial Q_i^2}+\tfrac{1}{2}M_i\omega_{ia}^2Q_i^2\right]\varphi_{a\alpha_i}(Q_i) = \epsilon_{a\alpha_i}\varphi_{a\alpha_i}(Q_i), \tag{2.7}$$

and is a harmonic-oscillator wave function.

We are interested in transitions from the ground state a to some excited state b. In order to evaluate Eq. (2.1) we will need vibrational wave functions for the excited state. These wave functions could be obtained in the same way as those for the ground state; but in general the Q_i will be different, since the symmetry of the excited electronic state, and hence of the adiabatic potential, differs from that of the ground state. Equation (2.1) will thus involve the evaluation of multidimensional integrals. In order to avoid this complication, we expand the adiabatic potential for the excited state b in the normal mode coordinates for the *ground state*

$$E_b(\mathbf{X})=E_{ab}+\sum_i A_iQ_i+\tfrac{1}{2}\sum_i M_i\omega_{ib}^2Q_i^2 + \sum_{i\neq j}V_{ij}Q_iQ_j. \tag{2.8}$$

If the last term in Eq. (2.8) were zero, the vibrational wave function for the excited state would be a product of harmonic oscillator functions of the Q_i, differing from the ground-state functions in their equilibrium positions, due to the appearance of the term linear in Q_i, and in their frequencies, due to the appearance of ω_{ib} instead of ω_{ia}.

The cross term in Q_i and Q_j causes a severe problem. In certain cases of high symmetry it may be shown to vanish, but in many cases of interest it will not. One method of dealing with this term is simply to assume that it is small and neglect it. A second method is to use the Hartree approximation to obtain a best set, in a variational sense, of functions in the form of a product of functions of the Q_i. We take as a trial solution to Eq. (2.2) for state b, with the adiabatic potential of Eq. (2.8),

$$\psi_{b\beta}(\mathbf{X})=\prod_i \varphi_{b\beta_i}(Q_i). \tag{2.9}$$

Using the variational principle[12] we find that the one-coordinate functions $\varphi_{b\beta_i}$ satisfy

$$\left\{-\frac{\hbar^2}{2M_i}\frac{\partial^2}{\partial Q_i^2}+\tfrac{1}{2}M_i\omega_{ib}^2Q_i^2+Q_i\left[A_i+\sum_{j\neq i}V_{ij}\int\varphi_{b\beta_j}^*(Q_j)\times Q_j\varphi_{b\beta_j}(Q_j)dQ_j\right]\right\}\varphi_{b\beta_i}(Q_i)=\epsilon_{b\beta_i}\varphi_{b\beta_i}(Q_i). \tag{2.10}$$

Equation (2.10) has the form of a harmonic-oscillator equation with displaced equilibrium. Thus by choosing a self-consistent set of displacements from equilibrium, we can obtain vibrational wave functions for the excited state which are a product of harmonic-oscillator functions (with changed equilibrium and frequency) in the ground-state normal coordinates. These functions will, of course, only be accurate if the cross term is not large; but they will certainly be better than those obtained by ignoring the cross term entirely.

Using the wave functions, Eqs. (2.6) and (2.9), the spectral representation of the δ function

$$\delta(E-E_0)=\frac{1}{2\pi\hbar}\int_{-\infty}^{\infty}dt\exp\left[-\frac{it}{\hbar}(E_0-E)\right], \tag{2.11}$$

and the fact that

$$\mathrm{Av}_a[f(p,q)]=\prod_i\left[1-\exp\left(-\frac{\epsilon_{a\alpha_i}}{kT}\right)\right]\times\sum_{\alpha_i}\exp\left(-\frac{\epsilon_{a\alpha_i}}{kT}\right)[f(p,q)] =\prod_i \mathrm{Av}_{\alpha_i}[f(p,q)], \tag{2.12}$$

the line-shape function, Eq. (2.1), may be written

$$I_{ab}(E)=\frac{1}{2\pi\hbar}\int_{-\infty}^{\infty}dt\exp\left[-\frac{it}{\hbar}(E-E_{ab})\right]\prod_i g_i(t), \tag{2.13}$$

where

$$g_i(t)=\mathrm{Av}_{\alpha_i}\sum_{\beta i}|\langle b\beta_i|a\alpha_i\rangle|^2\times\exp\left[-\frac{it}{\hbar}(\epsilon_{a\alpha_i}-\epsilon_{b\beta_i})\right]. \tag{2.14}$$

The Fourier transform of the line-shape function is a product of functions $g_i(t)$, which involve only the ith normal coordinate. Notice that $g_i(t)$ is just the Fourier transform of the line-shape function for the case in which only the ith mode is present. Thus we may compute a line-shape function for each mode independently and then obtain the total line-shape function by taking the Fourier inverse of the product of the individual mode Fourier transforms. Alternatively, the convolution theorem could be used to write Eq. (2.13) as an N-fold

[12] See, e.g., F. Seitz, *Modern Theory of Solids* (McGraw-Hill Book Company, Inc., New York, 1940), p. 677.

convolution,

$$I_{ab}(E)=\int\cdots\int I_{ab}^{(1)}(E_1)I_{ab}^{(2)}(E_2-E_1)\cdots \times I_{ab}^{(N)}(E-E_{N-1})dE_1\cdots dE_{N-1}, \quad (2.15)$$

where N is the total number of modes and $I_{ab}^{(i)}(E)$ is the line-shape function for mode i.

We may divide the vibrational modes into three types. First, there are modes for which the frequencies in the ground and excited states are the same, but the excited state adiabatic potential contains a term linear in the normal mode displacement. These linear modes will be treated in Sec. III. For normal coordinates of certain symmetries (e.g., odd-parity modes), the linear term in the excited state adiabatic potential will vanish, and the two adiabatic potentials can differ only in their frequencies. This second type of mode will be treated in Sec. IV. The third type of mode, which has both a linear term and a frequency change, will not be considered here.

B. General Features of Spectra

From Eq. (2.1) we see that the line-shape function consists of a number of δ functions, centered at various energies. We shall see that as more interacting vibrational modes of various frequencies are added, the average spacing between adjacent δ functions decreases, until ultimately the spacing becomes less than the bandwidth of the spectrometer, and the observed spectrum becomes continuous. A spectrometer set at an energy E actually sees the absorption over a range of energies from $E-\frac{1}{2}\Delta E$ to $E+\frac{1}{2}\Delta E$, where ΔE is the bandpass of the instrument. Thus to obtain the observed spectrum at E, we should add all of the weights of the δ functions in the range $E-\frac{1}{2}\Delta E$ to $E+\frac{1}{2}\Delta E$. This amounts to enfolding the δ-function spectrum with a square wave of unit height and width ΔE. More realistically, since the bandpass of a spectrometer is more like a Gaussian, we should convolute the δ-function spectrum with a Gaussian, whose width is the bandwidth of the instrument. Using this artifice, we obtain continuous spectra for comparison with experiment.

Of course this bandwidth effect is not the only source of broadening of the δ functions. We have assumed the validity of the adiabatic approximation and retained only harmonic terms in the adiabatic potentials. The vibrational levels of the ground and excited states are then stationary states of the system, neglecting the radiation field. In a real crystal, deviations from these approximations will give the phonon levels finite lifetimes and hence widths.

III. LINEAR MODES

In this section we will consider the line shape due to linear modes in the quantum theory and also in the semiclassical approximation.[4] Most of the results of this section are not new; however, we derive them from a somewhat different point of view, providing a useful introduction to the theory of quadratic modes. We take as the excited- and ground-state adiabatic potentials

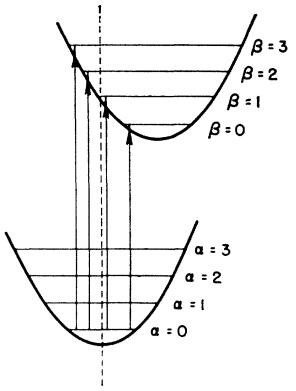

FIG. 1. Vibrational transitions for a linear mode at $T=0$. The transition with the lowest possible energy is $\alpha=0\rightarrow\beta=0$, and the line shape has a cutoff on the low-energy side.

$$E_b(q)=E_{ab}+a\hbar\omega(m\omega/\hbar)^{1/2}q+\tfrac{1}{2}m\omega^2q^2,$$
$$E_a(q)=\tfrac{1}{2}m\omega^2q^2. \quad (3.1)$$

q is the normal coordinate and a is a dimensionless constant which characterizes the size of the interaction. The solutions to Eq. (2.2) for the ground state are

$$\varphi_{a\alpha}(q)=\left[\frac{(m\omega/\hbar)^{1/2}}{\pi^{1/2}2^\alpha\alpha!}\right]^{1/2}e^{-\frac{1}{2}\rho^2}H_\alpha(\rho), \quad (3.2)$$

where $\rho=(m\omega/\hbar)^{1/2}q$ and $H_\alpha(z)$ is a Hermite polynomial.[13] The ground-state energies are

$$\epsilon_{a\alpha}=(\alpha+\tfrac{1}{2})\hbar\omega. \quad (3.3)$$

The solutions to Eq. (2.2) for the excited state are

$$\varphi_{b\beta}(q)=\left[\frac{(m\omega/\hbar)^{1/2}}{\pi^{1/2}2^\beta\beta!}\right]^{1/2}e^{-\frac{1}{2}(\rho+a)^2}H_\beta(\rho+a), \quad (3.4)$$

with energies

$$\epsilon_{b\beta}=(\beta+\tfrac{1}{2})\hbar\omega+E_{ab}-\frac{a^2}{2}\hbar\omega. \quad (3.5)$$

In order to compute the function (2.13), we wish to evaluate the overlap integral

$$S_{\alpha\beta}=\int\varphi_{a\alpha}(q)\varphi_{b\beta}(q)dq. \quad (3.6)$$

It is easily shown[14] that this integral is given by

$$S_{\alpha\beta}=e^{-a^2/4}\left[\frac{\alpha!}{\beta!}\right]^{1/2}\left(-\frac{a}{2^{1/2}}\right)^{\beta-\alpha}L_\alpha^{\beta-\alpha}\left(\frac{a^2}{2}\right). \quad (3.7)$$

[13] E. T. Copson, *Functions of a Complex Variable* (Oxford University Press, London, 1935), p. 271.
[14] T. H. Keil, thesis, University of Rochester (unpublished).

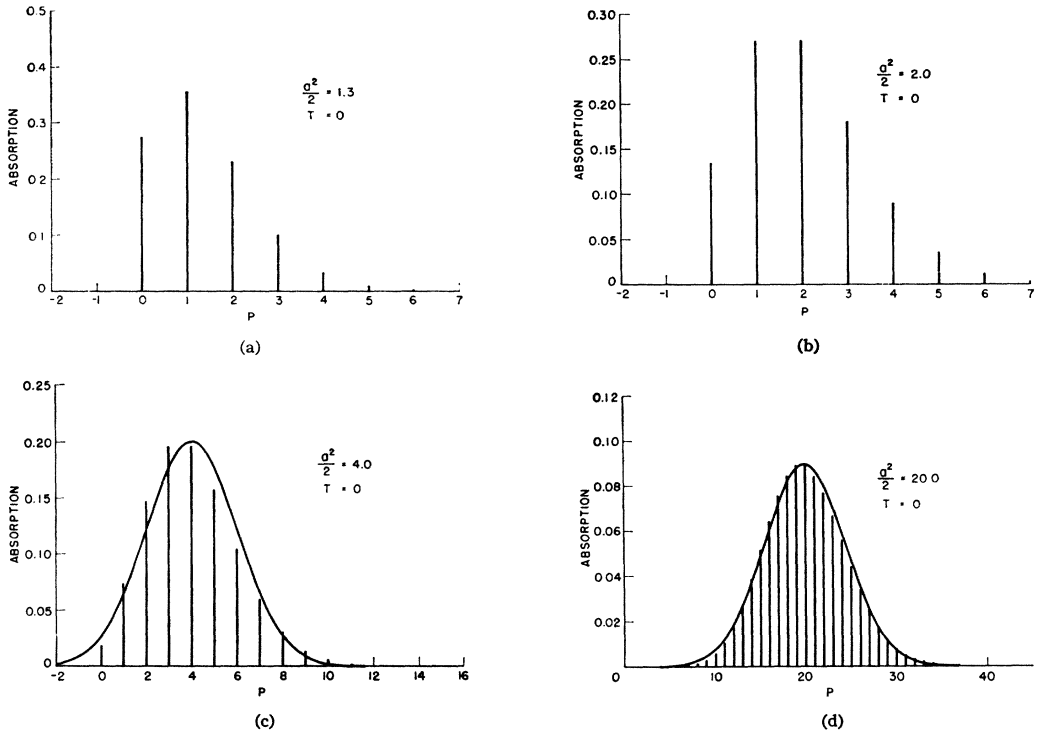

FIG. 2. The line shape due to a linear mode at $T=0$ for four values of the coupling constant: (a) $\frac{1}{2}a^2=1.3$, (b) $\frac{1}{2}a^2=2.0$, (c) $\frac{1}{2}a^2=4.0$, and (d) $\frac{1}{2}a^2=20.0$. The energy coordinate is $P=(E-E_{ab}+a^2\hbar\omega/2)/\hbar\omega$ [see Eq. (3.8)]. The continuous line in (c) and (d) is the semiclassical line shape.

The $L_n^m(z)$'s are Laguerre polynomials.[15] For $T=0$, only the $\alpha=0$ ground vibrational state is occupied and the line-shape function may easily be evaluated; using $L_0^m(z)=1$, and letting $p=\beta-\alpha$, we find

$$I_{ab}(E)=\sum_{p=0}^{\infty}\exp(-\tfrac{1}{2}a^2)((\tfrac{1}{2}a^2)^p/p!)\times\delta(p\hbar\omega+E_{ab}-\tfrac{1}{2}a^2\hbar\omega-E). \quad (3.8)$$

The line-shape function, Eq. (3.8), consists of a series of evenly spaced δ functions, with varying weights. The weights may be shown[2,16] to increase as p increases, reaching a maximum near $p=\frac{1}{2}a^2$ and then to decrease as p increases further. Note that the line shape, Eq. (3.8), has no contributions from negative p's; so there is a cutoff on the low-energy side of the absorption band. This occurs because, at $T=0$, only the $\alpha=0$ ground-state vibrational level is occupied, and the transition with the lowest possible energy from this state is $\alpha=0\rightarrow\beta=0$ (see Fig. 1), which gives $p=0$. For $\frac{1}{2}a^2$ large, this cutoff will not be important, since most of the absorption will be far away from the cutoff. Examples of linear mode line shapes at $T=0$ for four values of $\frac{1}{2}a^2$: $\frac{1}{2}a^2=1.3$, $\frac{1}{2}a^2=2.0$, $\frac{1}{2}a^2=4.0$ and $\frac{1}{2}a^2=20.0$ are shown in Figs. 2(a)–2(d). In these figures each δ function is plotted as a vertical line, with height equal to the weight of the δ function. The continuous curves in Figs. 2(c) and 2(d) are the semiclassical line shapes.

The linear mode line shape for arbitrary temperatures may also be evaluated. Since the ground- and excited-state frequencies are the same, the energy of a given vibrational transition depends only on the difference between excited- and ground-state vibrational quantum numbers. Hence, the thermal average may be performed in closed form with the aid of the identity[15]

$$\sum_{n=0}^{\infty}L_n^m(x)L_n^m(y)t^n n!/\Gamma(m+n+1)=\frac{(xyt)^{-m/2}}{1-t}\exp\left[-\frac{(x+y)t}{1-t}\right]I_m\left(\frac{2(xyt)^{1/2}}{1-t}\right), \quad (3.9)$$

where $I_m(z)$ is the Bessel function of the first kind with imaginary argument. The line-shape function becomes

$$I_{ab}(E)=\sum_{p=-\infty}^{\infty}\delta(p\hbar\omega+E_{ab}-\tfrac{1}{2}a^2\hbar\omega-E)\times\exp[(p\hbar\omega/2kT)-\tfrac{1}{2}a^2\coth(\hbar\omega/2kT)]\times I_p[\tfrac{1}{2}a^2\operatorname{csch}(\hbar\omega/2kT)]. \quad (3.10)$$

Examples of this line shape are shown in Figs. 3(a) to 3(c).

[15] E. T. Copson, Ref. 13, p. 270.
[16] J. J. Markham, Rev. Mod. Phys. 31, 956 (1959).

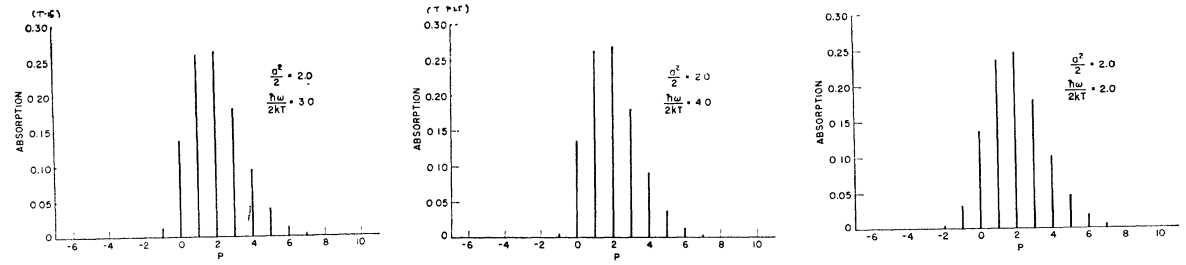

(a) (b) (c)

FIG. 3. The line shape due to a linear mode with $\frac{1}{2}a^2=2.0$ for three values of the temperature: (a) $\hbar\omega/2kT=2.0$, (b) $\hbar\omega/2kT=3.0$, and (c) $\hbar\omega/2kT=4.0$.

The semiclassical line shape[4] for a linear mode is given by

$$I_{ab}{}^{\text{s.c.}}(E)=\left[\frac{\tanh(\hbar\omega/2kT)}{\pi(a\hbar\omega)^2}\right]^{1/2}\times\exp\left[-(E-E_{ab})^2\frac{\tanh(\hbar\omega/2kT)}{(a\hbar\omega)^2}\right]. \quad (3.11)$$

It can be shown[4,16] that the line shape, Eq. (3.11), is a good approximation to the quantum line shape in two cases: first, if the frequency of the oscillator $\hbar\omega$ is small compared to the temperature kT, and second if the coupling constant a is large. In the first case both oscillators are treated classically, and in the second only the excited-state oscillator is treated classically. We will see in Sec. IV that for quadratic modes the large coupling case does not occur and the semiclassical approximation is correspondingly restricted. An example of the semiclassical line shape for large coupling is shown in Fig. 2(d).

IV. QUADRATIC MODES

A. Introduction

Thus far we have considered only the interaction of vibrational modes for which the difference between the excited- and ground-state adiabatic potentials is a constant plus a term linear in the normal mode displacement. If the impurity system possesses a center of inversion, symmetry dictates that the linear term vanish for odd-parity modes. In this case, the electron-lattice interaction will be dominated in the Condon approximation by the difference in frequency between the ground- and excited-state oscillators. The adiabatic potentials may be written

$$E_b(q)=E_{ab}+\tfrac{1}{2}m\omega_b{}^2q^2,\qquad E_a(q)=\tfrac{1}{2}m\omega_a{}^2q^2. \quad (4.1)$$

Discrete quadratic modes have previously been considered only in the semiclassical approximation.[17] We present here the first thorough quantum treatment of quadratic modes. In Parts B, C, and D we derive explicit expressions for the quantum line shape, first for zero temperature and then for arbitrary temperatures. In Part E we explore the semiclassical line shape and consider its validity and relation to the quantum line shape.

B. One Quadratic Mode, Zero Temperature

The solutions to Eq. (2.2) with the potentials of Eq. (4.1) for the ground and excited states are

$$\varphi_{a\alpha}(q)=\left[\frac{a}{\pi^{1/2}2^\alpha\alpha!}\right]^{1/2}e^{-a^2q^2/2}H_\alpha(aq),$$
$$\varphi_{b\beta}(q)=\left[\frac{b}{\pi^{1/2}2^\beta\beta!}\right]^{1/2}e^{-b^2q^2/2}H_\beta(bq), \quad (4.2)$$

where $a=(m\omega_a/\hbar)^{1/2}$ and $b=(m\omega_b/\hbar)^{1/2}$. The energies are

$$\epsilon_{a\alpha}=(\alpha+\tfrac{1}{2})\hbar\omega_a,\qquad \epsilon_{b\beta}=(\beta+\tfrac{1}{2})\hbar\omega_b+E_{ab}. \quad (4.3)$$

Using the density-matrix method of O'Rourke,[5] the line shape may be written as a Fourier integral

$$I_{ab}(\omega)=\frac{(\omega_a\omega_b)^{1/2}}{\pi}[1-\exp(-\beta_a)]\int_{-\infty}^{\infty}dt\,e^{-i\omega t}\times\{\Omega_+{}^2[1-\exp(-\beta_a-i\Omega_-t)]^2-\Omega_-{}^2[1-\exp(-\beta_a-i\Omega_+t)]^2\times\exp(2i\omega_bt)\}^{-1/2}, \quad (4.4)$$

where

$$\omega=(E-E_{ab})/\hbar+\tfrac{1}{2}\omega_a-\tfrac{1}{2}\omega_b,\qquad \beta_a=\hbar\omega_a/kT,\qquad \Omega_+{}^2=(\omega_a+\omega_b)^2,\qquad \Omega_-{}^2=(\omega_a-\omega_b)^2. \quad (4.5)$$

For zero temperature the line shape is

$$I_{ab}(\omega)=\frac{(\omega_a\omega_b)^{1/2}}{\pi}\times\int_{-\infty}^{\infty}dt\,e^{-i\omega t}[\Omega_+{}^2-\Omega_-{}^2\exp(2i\omega_bt)]^{-1/2}. \quad (4.6)$$

[17] Y. Toyozawa, Progr. Theoret. Phys. (Kyoto) **22**, 455 (1959).

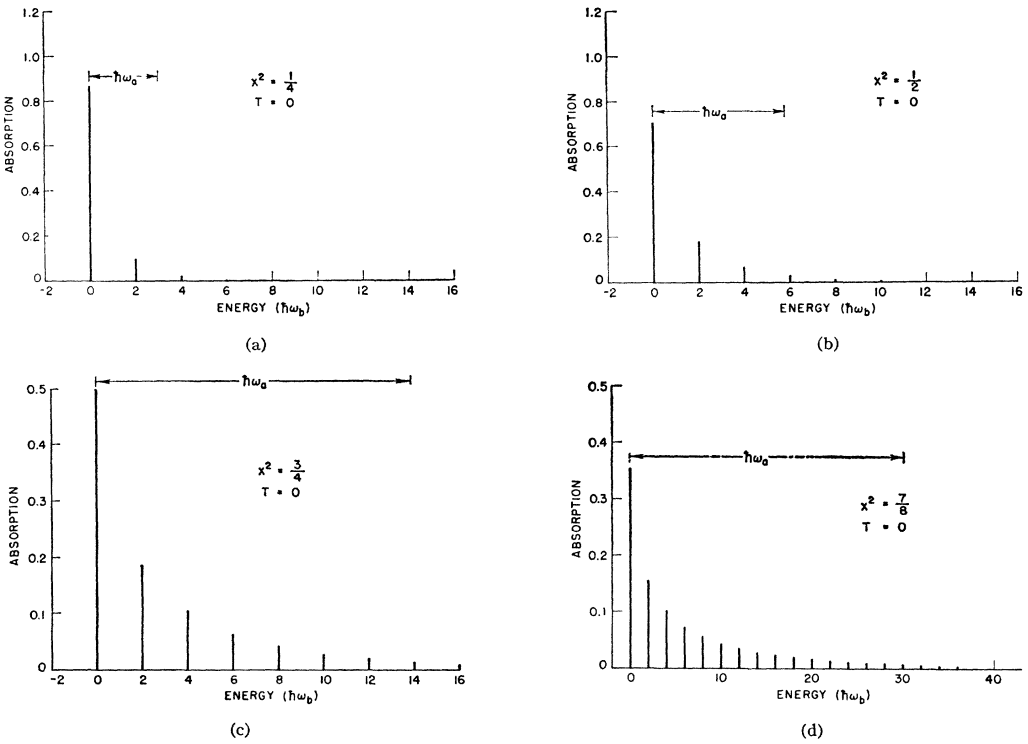

FIG. 4. The line shape due to a quadratic mode at $T=0$ for four values of the coupling constant $x^2=(\omega_b-\omega_a)^2/(\omega_b+\omega_a)^2$: (a) $x^2=\frac{1}{4}$, (b) $x^2=\frac{1}{2}$, (c) $x^2=\frac{3}{4}$, (d) $x^2=\frac{7}{8}$. The energy coordinate is $\hbar\omega$ [see Eq. (4.5)] plotted in units of $\hbar\omega_b$.

Expanding the factor in brackets in a power series in $\exp(2i\omega_b t)$ and using Eq. (2.11), the line-shape function becomes

$$I_{ab}(\omega)=\frac{(\omega_a\omega_b)^{1/2}}{\omega_a+\omega_b}\sum_{l=0}^{\infty}\delta(2l\omega_b-\omega)\times\frac{2l!}{2^{2l}(l!)^2}\left(\frac{\omega_a-\omega_b}{\omega_a+\omega_b}\right)^{2l}. \quad (4.7)$$

Equation (4.7) consists of a series of equally spaced δ functions with spacing twice the excited-state vibrational frequency. The quantities $2l!/2^{2l}(l!)^2$ for the first few values of l are listed in Table I.

Inspection of Table I shows that for all admissible values of the parameter

$$x^2=(\omega_b-\omega_a)^2/(\omega_b+\omega_a)^2\leq 1, \quad (4.8)$$

the weights of the δ functions decrease monotonically with increasing l. Thus the peak of the line shape is always at $l=0$ ($\omega=0$). No absorption appears on the low-energy side of $\omega=0$ and the line shape has a tail on the high-energy side regardless of whether the excited- or ground-state frequency is larger. Using Stirling's formula it can be shown that the weight function decreases like $l^{-1/2}\exp(-Cl)$ for large l (C is a constant). The sharp cutoff on the low-energy side at $T=0$ results from the fact that only the $\alpha=0$ state is occupied, and the transition with the lowest possible energy is $\alpha=0\rightarrow\beta=0$.

TABLE I. Weight functions for one- and three-dimensional quadratic modes.

l	$2l!/2^{2l}(l!)^2$	$(2l+1)!/2^{2l}(l!)^2$
0	1	1
1	1/2=0.500	3/2=1.50
2	3/8=0.375	15/8=1.88
3	5/16=0.312	35/16=2.08
4	35/128=0.274	315/128=2.46
5	63/256=0.245	693/256=2.71
6	231/1024=0.221	3003/1024=2.93

Figures 4(a)–4(d) give examples of the line-shape function, Eq. (4.7). The zero of energy is given by $\hbar\omega=0$ [see Eq. 4.5)] and the energy is in units of the excited-state vibrational frequency $\hbar\omega_b$. With x^2 defined in Eq. (4.8), Fig. 4(a) corresponds to $x^2=\frac{1}{4}$, Fig. 4(b) to $x^2=\frac{1}{2}$, Fig. 4(c) to $x^2=\frac{3}{4}$, and Fig. 4(d) to $x^2=\frac{7}{8}$. $\hbar\omega_a$ is plotted as a barred line in each figure. The half-width of the line-shape function occurs, from Table I, when $0\leq l\leq 1$. Thus the half-width is on the order of the excited-state vibrational frequency.

The energy variable $\hbar\omega$ is defined with respect to the difference in zero-point energy of the ground- and excited-state oscillators [see Eq. (4.5)]. Since the peak of the absorption lies at $\hbar\omega=0$, changing this difference

(e.g., by changing the mass of the oscillators) shifts the peak. This is in direct contrast to the linear mode case, where changing the oscillator mass does not shift the peak. The peak shift for a quadratic mode is given by

$$\Delta \text{ peak} = \tfrac{1}{2}[1-(m/m')^{1/2}]\hbar(\omega_a-\omega_b), \quad (4.9)$$

where m is the original mass and m' the new (ω_a and ω_b are the original frequencies), and Δ peak is taken as positive if the shift is to higher energy.

We also expect a change in the half-width with a change in the oscillator mass. The weights of the δ functions do not change with a change in mass. Hence the change in width is due only to the change in $\hbar\omega_b$, and we may write the ratio of the half-widths as

$$W_m/W_{m'} = (m'/m)^{1/2}. \quad (4.10)$$

The corresponding expression for a linear mode at $T=0$ contains a fourth root instead of a square root.[18] Both the peak shift and width change are expected to be sensitive to temperature since the mass appears in $\hbar\omega_a/kT$.

For completeness we give the first three moments of Eq. (4.7)

$$\begin{aligned} M^{(1)} &= \hbar\omega_b(\omega_a-\omega_b)^2/4\omega_a\omega_b, \\ m^{(2)} &= (\hbar\omega_b)^2(\omega_a^2-\omega_b^2)/8\omega_a^2\omega_b^2, \\ m^{(3)} &= (\hbar\omega_b)^3(\omega_a^2-\omega_b^2)^2(\omega_a^2+\omega_b^2)/8\omega_a^3\omega_b^3. \end{aligned} \quad (4.11)$$

Here

$$M^{(N)} = \int I_{ab}(\omega)(\hbar\omega)^N d(\hbar\omega)$$

and

$$m^{(N)} = \int I_{ab}(\omega)(\hbar\omega - M^{(1)})^N d(\hbar\omega).$$

For quadratic modes the line shape is highly asymmetric and the first moment has little relation to the peak of the absorption.

Finally we consider the case for which $\omega_b \ll \omega_a$. We expand Eq. (4.6) in the small quantity ω_b/ω_a and keep only lowest order terms, that is

$$\begin{aligned} \Omega_+^2 &= \omega_a^2+2\omega_a\omega_b, \\ \Omega_-^2 &= \omega_a^2-2\omega_a\omega_b, \\ \exp(2i\omega_b t) &= 1+2i\omega_b t. \end{aligned} \quad (4.12)$$

The line-shape function becomes

$$I_{ab}(\omega) = \frac{1}{\pi}(2\omega_a)^{-1/2}\int_{-\infty}^{\infty} dt\, e^{-i\omega t}[2/\omega_a - it]^{-1/2}.$$

The integral may be performed[19] and the line shape is

$$I_{ab}(\omega) = \begin{cases} \pi^{-1/2}(2/\omega_a)^{1/2}\omega^{-1/2}\exp(-2\omega/\omega_a) & (\omega>0) \\ 0 & (\omega<0). \end{cases} \quad (4.13)$$

Here, $\omega = (E-E_{ab})/\hbar + \frac{1}{2}\omega_a$. Thus for $\omega_b \ll \omega_a$ the discrete line shape goes over into a continuous curve. The absorption has a sharp cutoff on the low-energy side, with absorption beginning at $E = E_{ab} - \frac{1}{2}\hbar\omega_a$ and decreasing exponentially as E increases further.

It may seem surprising that, for zero frequency in the excited state, the line shape should become a continuous function of energy with finite width. Inspection of Figs. 4(a) to 4(d) shows that as x^2 becomes close to one (which means, for ω_a fixed, as ω_b tends to zero), the ground-state vibrational functions overlap appreciably with a larger number of excited-state vibrational functions. Roughly, this number increases linearly with ω_a/ω_b, and becomes large as $\omega_b \to 0$. At the same time, the spacing between excited vibrational states decreases like ω_b/ω_a. In the limit these two effects "cancel" and the line shape (4.13) is obtained.

C. Degenerate Quadratic Modes, Zero Temperature

In a real crystal, two- and three-fold degenerate (as well as nondegenerate) vibrations may be present. Hence it is of interest to examine the line shapes due to multidimensional quadratic modes. First we consider two quadratic modes, where the two ground-state frequencies are ω_a and the two excited-state frequencies are ω_b. From Eqs. (2.13) and (4.6) the line shape is

$$I_{ab}(\omega) = \frac{\omega_a\omega_b}{\pi}\int_{-\infty}^{\infty} dt\, e^{-i\omega t}[\Omega_+^2 - \Omega_-^2\exp(2i\omega_b t)]^{-1}, \quad (4.14)$$

where $\omega = (E-E_{ab})/\hbar + \omega_a - \omega_b$. Proceeding as before, we obtain

$$I_{ab}(\omega) = \frac{4\omega_a\omega_b}{(\omega_a+\omega_b)^2}\sum_{l=0}^{\infty}\delta(2l\omega_b-\omega)\left(\frac{\omega_a-\omega_b}{\omega_a+\omega_b}\right)^{2l}. \quad (4.15)$$

The first three moments of Eq. (4.15) are just twice the corresponding single-mode moments, Eq. (4.11).[20] This simple additivity does not apply for higher moments. The general features of the two-dimensional quadratic mode line shape are similar to those of the one-dimensional line shape. The absorption is generally broader, but the peak is still at $\hbar\omega=0$, and the sharp cutoff on the low-energy side and the high-energy tail are still present.

Next we consider three quadratic modes, where the three ground-state frequencies are ω_a and the three excited-state frequencies are ω_b. The line shape is now

$$I_{ab}(\omega) = \frac{(\omega_a\omega_b)^{3/2}}{\pi} \times \int_{-\infty}^{\infty} dt\, e^{-i\omega t}[\Omega_+^2 - \Omega_-^2\exp(2i\omega_b t)]^{-3/2}, \quad (4.16)$$

[18] C. C. Klick and J. H. Schulman, *Solid State Physics*, edited by F. Seitz and D. Turnbull (Academic Press Inc., New York, 1957), Vol. 5.

[19] *Bateman Manuscript Project, Tables of Integral Transforms*, edited by H. Erdelyi (McGraw-Hill Book Company, Inc., New York, 1954), Vol. 1, p. 119.

[20] A. Gold and T. H. Keil (to be published); see also Ref. 14.

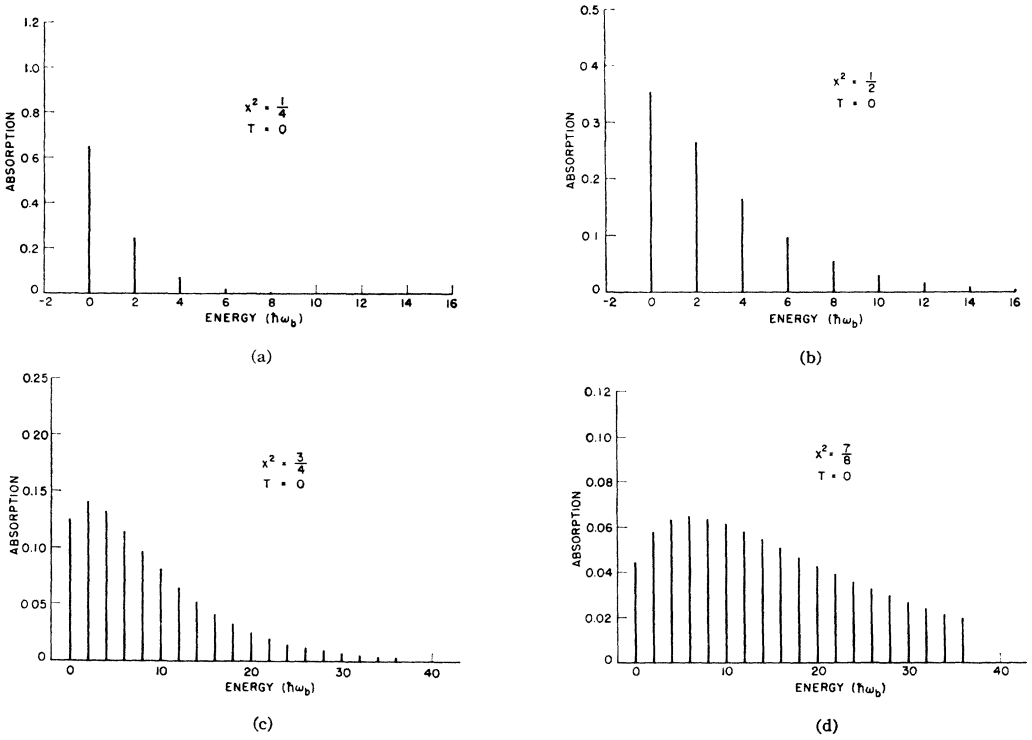

FIG. 5. The line shape due to a threefold degenerate quadratic mode for four values of the coupling constant: (a) $x^2=\frac{1}{4}$, (b) $x^2=\frac{1}{2}$, (c) $x^2=\frac{3}{4}$, (d) $x^2=\frac{7}{8}$. The energy coordinate is $\hbar\omega$, plotted in units of $\hbar\omega_b$.

where $\omega=(E-E_{ab})/\hbar+3\omega_a/2-3\omega_b/2$; and in terms of δ functions

$$I_{ab}(\omega)=\frac{8(\omega_a\omega_b)^{3/2}}{(\omega_a+\omega_b)^3}\sum_{l=0}^{\infty}\delta(2l\omega_b-\omega)\times\frac{(2l+1)!}{2^{2l}(l!)^2}\left(\frac{\omega_a-\omega_b}{\omega_a+\omega_b}\right)^{2l}. \quad (4.17)$$

The first few coefficients $(2l+1)!/2^{2l}(l!)^2$ are listed in Table I. The first three moments of Eq. (4.17) are given by three times the corresponding single-mode moments, Eq. (4.11).[20]

In Figs. 5(a) through 5(d) we have plotted Eq. (4.17) for four values of x^2: $x^2=\frac{1}{4}$, $x^2=\frac{1}{2}$, $x^2=\frac{3}{4}$, and $x^2=\frac{7}{8}$. Again the absorption is broader than for a single mode, and a low-energy cutoff and high-energy tail appear. One new feature appears; for $x^2>\frac{2}{3}$, the lowest energy, $\omega=0$ peak is no longer the highest. Inspection of Table I shows that the peak will be pushed to higher energies (in units of $\hbar\omega_b$) as x^2 becomes closer to one.

Methods for treating more complicated cases of degeneracy (e.g., if the degeneracies for the ground and excited states are different) will be developed in Sec. V.

D. Quadratic Modes, Finite Temperatures

1. General Considerations

The essential complication for quadratic modes at finite temperatures is that the energy of a given transition does not depend solely on the difference between ground- and excited-state vibrational quantum numbers. Because of this, the line shape becomes significantly more complicated and can no longer be expressed in a simple form. The most convenient way to calculate the line shape is to let a digital computer do most of the work. We have written a computer program[21] which calculates the line shape and, with the aid of a digital plotter, draws this line shape on graph paper. For the relatively complicated line shapes considered here, such methods are essential.

The moments of Eq. (4.4) are easily obtained, and before proceeding to calculate the line shape we tabulate the first three moments,

$$\begin{aligned}M^{(1)}&=\hbar\{(\omega_a-\omega_b)^2+(\omega_a{}^2-\omega_b{}^2)\times[1-\coth(\hbar\omega_a/2kT)]\}/4\omega_a,\\ m^{(2)}&=\hbar^2(\omega_a{}^2-\omega_b{}^2)^2\coth^2(\hbar\omega_a/2kT)/8\omega_a{}^2,\\ m^{(3)}&=\hbar^3(\omega_a{}^2-\omega_b{}^2)^2[2\omega_a{}^2\coth(\hbar\omega_a/2kT)+(\omega_b{}^2-\omega_a{}^2)\coth^3(\hbar\omega_a/2kT)]/8\omega_a{}^3.\end{aligned} \quad (4.18)$$

$M^{(1)}$ is again measured with respect to $\hbar\omega=0$.

The calculation of the line shape begins with Eq. (2.1)

$$I_{ab}(\hbar\omega)=[1-\exp(-\hbar\omega_a/kT)]\sum_{\alpha}\exp(-\alpha\hbar\omega_a/kT)\times\sum_{\beta}|S_{\alpha\beta}|^2\delta(\beta\hbar\omega_b-\alpha\hbar\omega_a-\hbar\omega), \quad (4.19)$$

[21] T. H. Keil, report, University of Rochester, 1965 (unpublished).

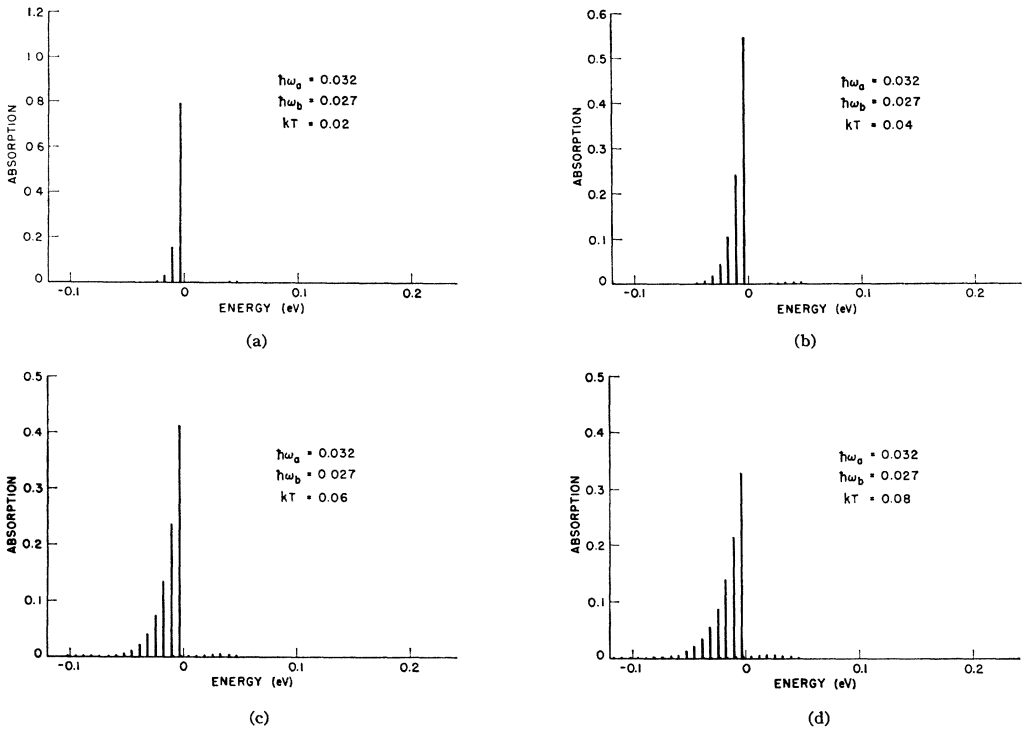

FIG. 6. The line shape due to a quadratic mode with $\omega_a \approx \omega_b$ for four temperatures: (a) $kT=0.02$, (b) $kT=0.04$, (c) $kT=0.06$, and (d) $kT=0.08$. The frequencies are $\hbar\omega_a=0.032$ and $\hbar\omega_b=0.027$. The energy coordinate is $E-E_{ab}$; the energy units are arbitrary.

where

$$S_{\alpha\beta}=\int \varphi_{a\alpha}(q)\varphi_{b\beta}(q)dq. \tag{4.20}$$

$\varphi_{a\alpha}(q)$ and $\varphi_{b\beta}(q)$ are defined by Eq. (4.2), and ω by Eq. (4.5). In Appendix A we develop several expressions for $S_{\alpha\beta}$, the most compact of which is

$$S_{\alpha\beta}=\left[\frac{(1-x^2)^{1/2}}{2x}\right]^{1/2}\frac{(-1)^{\alpha/4-\beta/4+1/4}}{(\alpha!\beta!)^{1/2}} \times P_{\alpha/2-\beta/2+1/2}{}^{\alpha/2+\beta/2+1/2}\left(i\frac{(1-x^2)^{1/2}}{x}\right), \tag{4.21}$$

where $x=(\omega_b-\omega_a)/(\omega_b+\omega_a)$, and $P_\nu{}^\mu(iz)$ is the associated Legendre function.[22] The selection rules are contained in the factor $P_\nu{}^\mu(iz)$. For μ and ν half integers, $P_\nu{}^\mu$ is a polynomial in z. For μ and ν integers, $P_\nu{}^\mu$ is identically zero. Thus $S_{\alpha\beta}$ will be nonzero when α and β are either both even or both odd, and zero otherwise. This is just a consequence of the parity of the vibrational states.

2. *A Simple Case:* $\omega_a \approx \omega_b$

One simple case is immediately suggested. If the ground- and excited-state frequencies are nearly equal, we expect that most of the contribution to the overlap integrals occurs for $\alpha=\beta$. It can be shown[14] that, for $\omega_b \approx \omega_a$

$$S_{\alpha\alpha}=1-\tfrac{1}{4}x^2(\alpha^2+\alpha+1). \tag{4.22}$$

Assuming that terms of $O(x^2)$ may be neglected, Eq. (4.19) becomes

$$I_{ab}(\hbar\omega)=[1-\exp(-\hbar\omega_a/kT)]\sum_\alpha \exp(-\alpha\hbar\omega_a/kT) \times\delta[\alpha(\hbar\omega_b-\hbar\omega_a)-\hbar\omega]. \tag{4.23}$$

Equation (4.23) is a series of equally spaced δ functions, with spacing $\hbar(\omega_a-\omega_b)[\sim O(x)]$, whose weights simply reflect the Boltzmann distribution of oscillators in the electronic ground state [at $T=0$, Eq. (4.23) becomes a single δ function at $\hbar\omega=0$]. The largest δ function occurs for $\alpha=0(\hbar\omega=0)$ and the others fall on the low-energy side of $\hbar\omega=0$ if $\omega_a>\omega_b$ and on the high-energy side if $\omega_b>\omega_a$.

In Figs. 6(a) through 6(d) examples of the line-shape function, Eq. (4.23), are plotted. In these figures the energy coordinate is $E-E_{ab}$. In all four figures the frequencies are $\hbar\omega_a=0.032$ and $\hbar\omega_b=0.027$; the temperature varies from $kT=0.02$ to $kT=0.08$. The energy units are arbitrary (but the sizes of the numbers are chosen to correspond roughly to electron volts). The additional structure to the high-energy side of the $\hbar\omega=0$ peak in Figs. 6(c) and 6(d) is due to that fact that for

[22] See Ref. 13, p. 272.

the frequencies chosen $\omega_b \approx \omega_a$ is not a very good approximation.

Notice that there is in some sense a competition between making $|\omega_b - \omega_a|$ small enough so that x^2 is negligible and the consequent reduction in the total width of the line shape necessitated by the reduction in the spacing between δ functions. Rewriting the first moment Eq. (4.18) in terms of x, neglecting terms of $O(x^2)$

$$M^{(1)} = -\hbar x \omega_a [1 - \coth(\hbar\omega_a/2kT)]. \quad (4.24)$$

For reasonable temperatures $\coth(\hbar\omega_a/2kT)$ may range between 1 and 10; so that the center of gravity, which roughly gives the width, never gets more than a few $\hbar\omega_a$ away from $\hbar\omega = 0$. For very high temperatures $\coth(\hbar\omega_a/2kT) \sim 2kT/\hbar\omega_a$, and the first moment becomes

$$M^{(1)} = 2xkT, \quad (4.25)$$

and the center of gravity is imited to a fraction of kT. Thus the total width is essentially limited to $\hbar\omega_a$ or kT, whichever is larger.

3. General Values of the Frequencies

For the general case it is instructive to rewrite Eq. (4.19) as

$$I_{ab}(\hbar\omega) = [1 - \exp(-\hbar\omega_a/kT)]\{\sum_\beta |S_{0,2\beta}|^2 \delta(2\beta\hbar\omega_b - \hbar\omega) + \sum_\beta \exp(-\hbar\omega_a/kT)|S_{1,2\beta+1}|^2$$
$$\times \delta[2\beta\hbar\omega_b - (\hbar\omega_a - \hbar\omega_b) - \hbar\omega] + \sum_\beta \exp(-2\hbar\omega_a/kT)|S_{2,2\beta}|^2 \delta(2\beta\hbar\omega_b - 2\hbar\omega_a - \hbar\omega)$$
$$+ \sum_\beta \exp(-3\hbar\omega_a/kT)|S_{3,3\beta+1}|^2 \delta[2\beta\hbar\omega_b - (3\hbar\omega_a - \hbar\omega_b) - \hbar\omega] + \cdots\}. \quad (4.26)$$

Each term consists of a series of equally spaced δ functions at intervals of $2\hbar\omega_b$, with the first δ function from each term located at an energy given by

$$\begin{aligned} \hbar\omega &= -\alpha\hbar\omega_a \quad (\alpha \text{ even}), \\ \hbar\omega &= -(\alpha\hbar\omega_a - \hbar\omega_b) \quad (\alpha \text{ odd}). \end{aligned} \quad (4.27)$$

The successive δ functions extend toward higher energy.

In Figs. 7(a) and 7(b) we have plotted examples of finite-temperature quadratic modes. In both the energy variable is $E - E_{ab}$, the ground-state frequency is $\hbar\omega_a = 0.0138$, and the excited-state frequency is $\hbar\omega_b = 0.001$ (which gives $x^2 = \frac{3}{4}$). In Fig. 7(a) the temperature is $kT = 0.03$ and in Fig. 7(b) $kT = 0.04$. In Fig. 7(a) the first δ function of each term in Eq. (4.26) is marked by a pair of numbers (α,β), the ground- and excited-state vibrational quantum numbers, respectively. As the temperature increases we expect the $\alpha = 0$ transitions [from the first term of Eq. (4.26)] to become relatively less important and transitions for higher values of α to increase in importance. Inspection of Fig. 7(b) shows that this is the case. The continuous curve in Fig. 7(b) is the semiclassical line shape which will be discussed later.

For computer analysis it is convenient to write Eq. (4.19) in a somewhat different form. Assume that there exist integers n_a and n_b, such that

$$n_a\omega_a = n_b\omega_b. \quad (4.28)$$

The argument of the δ function in Eq. (4.19) can be rewritten as

$$\beta\hbar\omega_b - \alpha\hbar\omega_a - \hbar\omega = (\beta n_a - \alpha n_b)\hbar\omega_b/n_a - \hbar\omega. \quad (4.29)$$

We now define the integer $\gamma = \beta n_a - \alpha n_b$ and rewrite Eq. (4.19) by converting the sum over α and β to a sum over γ and α:

$$I_{ab}(\hbar\omega) = [1 - \exp(-\hbar\omega_a/kT)]$$
$$\times \sum_{\gamma=-\infty}^{\infty} \sum_\alpha{}' \exp(-\alpha\hbar\omega_a/kT)$$
$$\times |S_{\alpha\beta}|^2 \delta(\gamma\hbar\omega_a/n_a - \hbar\omega), \quad (4.30)$$

where $\sum_\alpha{}'$ means sum over those α such that, with γ fixed, $\beta = (\gamma + \alpha n_b)/n_a$ is an integer.

Hence in Eq. (4.30) we have obtained a series of evenly spaced δ functions (spacing $\hbar\omega_b/n_a$), indexed by γ, each of whose weight is given by

$$P(\gamma) = [1 - \exp(-\hbar\omega_a/kT)]$$
$$\times \sum_\alpha{}' \exp(-\alpha\hbar\omega_a/kT)|S_{\alpha\beta}|^2; \quad (4.31)$$

and the line shape may be written

$$I_{ab}(\hbar\omega) = \sum_{\gamma=-\infty}^{\infty} P(\gamma)\delta(\gamma\hbar\omega_b/n_a - \hbar\omega). \quad (4.32)$$

4. The Limiting Case: $\omega_b \ll \omega_a$

Finally, we consider the case for which $\omega_b \ll \omega_a$. As in the zero-temperature case, the line shape in the limit goes from a discrete series of lines to a continuous line shape. Working with the line shape in the form of Eq. (4.4), expanding in the small quantity ω_b/ω_a, and

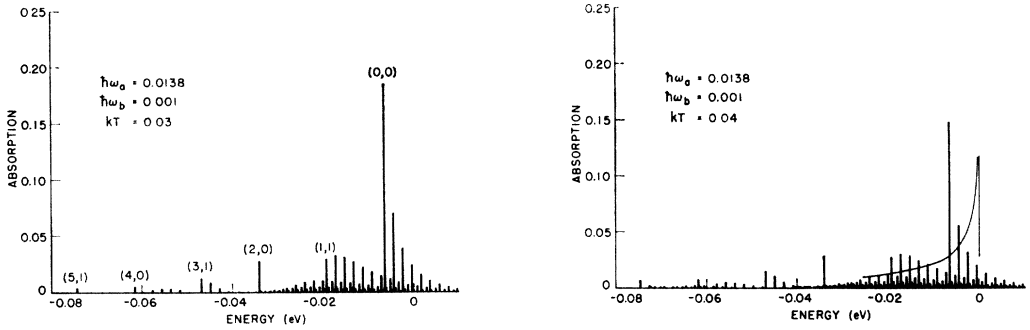

FIG. 7. The line shape due to a quadratic mode with $\hbar\omega_a=0.0138$ and $\hbar\omega_b=0.001$ for two temperatures: (a) $kT=0.03$ and (b) $kT=0.04$. The energy coordinate is $E-E_{ab}$; the energy units are arbitrary. The continuous line in (b) is the semiclassical line shape.

using Eq. (4.12), we obtain, for $\omega_b \ll \omega_a$

$$I_{ab}(\omega)=\frac{1}{2\pi}[1-\exp(-\beta_a)] \times\int_{-\infty}^{\infty} dt e^{-i\omega t}[1-\exp(-\beta_a-i\omega_a t)]^{-1/2} \times[(1-\tfrac{1}{2}i\omega_a t)-(1+\tfrac{1}{2}i\omega_a t) \times\exp(-\beta_a-i\omega_a t)]^{-1/2}. \quad (4.33)$$

Here, $\omega=(E-E_{ab})/\hbar+\frac{1}{2}\omega_a$. The integral may be performed, and, as is shown in Appendix B, the line shape is

$$I_{ab}(\omega)=(2/\pi^2\omega_a)^{1/2}[1-\exp(-\beta_a)]\sum_{\alpha=0}^{\infty}(\omega+\alpha\omega)^{-1/2} \times\exp(-\alpha\beta_a)\exp[-2(\omega+\alpha\omega_a)/\omega_a] \times f_\alpha[4(\omega+\alpha\omega_a)/\omega_a], \quad (4.34)$$

where

$$f_\alpha(z)=\sum_{m=0}^{\alpha}\frac{\Gamma(m+\frac{1}{2})}{m!}(-1)^{\alpha-m}L_{\alpha-m}^{-1/2}(z) \quad (z>0) =0 \quad (z<0). \quad (4.35)$$

$L_n^{-1/2}(z)$ is the associated Laguerre function. $f_\alpha(z)$ is a polynomial of degree α in z. The first few $f_\alpha(z)$ are given by Eq. (B6) of Appendix B.

The line shape, Eq. (4.34), consists of a series of terms, each of which is associated with a particular value of α, the ground-state quantum number. For α even, the leading term in $f_\alpha(z)$ is a constant, so Eq. (4.34) has singularities at $\omega=-\alpha\omega_a$ (α even), due to the $(\omega+\alpha\omega_a)^{-1/2}$ dependence. Thus the line shape has a series of sharp peaks, with spacing $2\hbar\omega_a$, extending towards lower energy, superimposed on a broad continuous background. Such a line shape is shown in Fig. 8, where $\hbar\omega_a=0.02$ and $kT=0.04$. Physically one might expect to see such a line shape if the ground state of the impurity is very well localized, and couples strongly to the vibrational mode in question; while the excited state of the impurity is very diffuse and couples only weakly to that mode.

E. Quadratic Modes, Semiclassical

The semiclassical line-shape function for a quadratic mode is easily calculated, using the methods of Ref. 4. We obtain, for $\omega_b<\omega_a$

$$I_{ab}^{\text{s.c.}}(E')=-\frac{1}{\pi^{1/2}}\left[\frac{2\omega_a\tanh(\hbar\omega_a/2kT)}{\hbar(\omega_b^2-\omega_a^2)}\right]^{1/2}E'^{-1/2}\exp\left[-\frac{2E'\omega_a\tanh(\hbar\omega_a/2kT)}{\hbar(\omega_b^2-\omega_a^2)}\right] \quad (E'<0) =0 \quad (E'>0), \quad (4.36)$$

and for $\omega_b>\omega_a$

$$I_{ab}^{\text{s.c.}}(E')=0 \quad (E'<0) =\frac{1}{\pi^{1/2}}\left[\frac{2\omega_a\tanh(\hbar\omega_a/2kT)}{\hbar(\omega_b^2-\omega_a^2)}\right]^{1/2}E'^{-1/2}\exp\left[-\frac{2E'\omega_a\tanh(\hbar\omega_a/2kT)}{\hbar(\omega_b^2-\omega_a^2)}\right] \quad (E'>0). \quad (4.37)$$

Here $E'=E-E_{ab}$.

Equation (4.36) for $\omega_b<\omega_a$, shows an exponentially decreasing energy dependence to the low-energy side of $E'=0$ and a sharp cutoff on the high-energy side, even at $T=0$. This is in direct contrast to the quantum result at $T=0$, Eq. (4.7), which has a high-energy tail

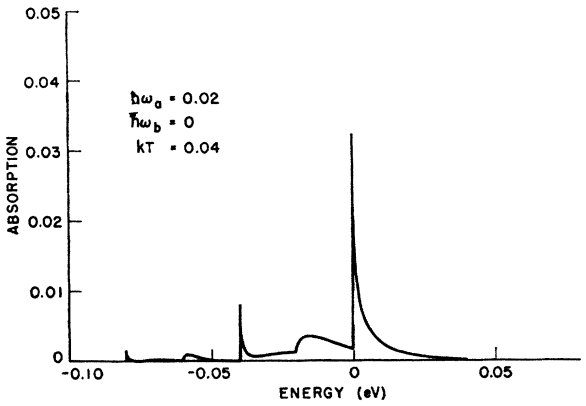

FIG. 8. The line shape due to a quadratic mode with $\hbar\omega_a=0.02$, $\hbar\omega_b=0.0$, and $kT=0.04$. The energy coordinate is $\hbar\omega$ [see Eq. (4.33)].

and a low-energy cutoff. In Fig. 9(a) we have plotted Eq. (4.36) for $T=0$ and $\omega_a=3\omega_b$, together with the corresponding quantum line shape. In Fig. 9(b) we have plotted the same thing but with $\omega_a=13.9\ \omega_b$. The energy variable here is $\hbar\omega$ [see Eq. (4.5)] and is in units of $\hbar\omega_b$. The contrast is quite striking. Clearly the semiclassical approximation is not very good for $T=0$ and $\omega_b<\omega_a$.

It is easily shown that the first two moments of Eq. (4.36) are identical to the corresponding quantum moments Eq. (4.18). Hence even though the quantum and semiclassical line shapes are as different as shown in Figs. 8(a) and 8(b) the first two moments are identical. This is an excellent example of the care which must be taken when using moments.[14]

The semiclassical approximation consists of neglecting the commutator of the excited- and ground-state vibrational Hamiltonians.[4] This commutator is given by

$$[H_b,H_a]=\tfrac{1}{2}\hbar^2(\omega_b^2-\omega_a^2)(1+q\partial/\partial q). \quad (4.38)$$

When Eq. (4.38) is zero, the argument of the exponential in Eqs. (4.36) and (4.37) is singular. The interesting case is, therefore, that for which the commutator $[H_b,H_a]$ is zero, while the argument of the exponentials remains finite. For $\hbar\omega_a\ll kT$, $\tanh(\hbar\omega_a/2kT)\approx\hbar\omega_a/2kT$, and the argument of the exponential becomes $[-(E'/kT)/\omega_a^2/(\omega_b^2-\omega_a^2)]$. We wish to have $\omega_a^2/(\omega_b^2-\omega_a^2)$ finite while $\omega_b^2-\omega_a^2=0$. This implies that both frequencies are small (the case for which $\omega_a=\omega_b$ is trivial: both quantum and semiclassical methods lead to a single δ function at $E'=0$).

The connection between the quantum and semiclassical results may be established by working with Eq. (4.4) for the quantum line shape. Expanding in the small quantities ω_a and ω_b, and retaining only lowest order terms, we obtain

$$I_{ab}(E')=\frac{1}{2\pi\hbar}\left[\frac{\omega_a^2}{(kT|\omega_b^2-\omega_a^2|)}\right]^{1/2}\int_{-\infty}^{\infty}\exp\left(\frac{-iE't}{\hbar}\right)\left[\frac{\hbar\omega_a^2}{(kT|\omega_b^2-\omega_a^2|)}\pm it\right]^{-1/2}dt. \quad (4.39)$$

The plus sign applies for $\omega_b<\omega_a$ and the minus sign for $\omega_a<\omega_b$. The integral may be performed[19] and

$$\begin{aligned}I_{ab}(E')&=\mp\pi^{-1/2}\{\omega_a^2/[kT(\omega_b^2-\omega_a^2)]\}^{1/2}E'^{-1/2}\exp[-(E'/kT)\omega_a^2/(\omega_b^2-\omega_a^2)] \quad (E'\lesseqgtr 0;\ \omega_b\lesseqgtr\omega_a)\\ &=0 \quad (E'\gtreqless 0;\ \omega_b\gtreqless\omega_a).\end{aligned} \quad (4.40)$$

This result is in agreement with Eqs. (4.36) and (4.37) if $\hbar\omega_a\ll kT$.

Thus, the semiclassical approximation for a quadratic mode will be valid for small frequencies ω_a and ω_b and for temperatures large compared to the ground-state frequency ω_a. For a linear mode we found that the semiclassical approximation was valid for small frequency and large temperature, but in addition the semiclassical line shape gave a good approximation to the envelope of the line shape for large coupling ($a^2/2\gg1$). The approximation failed completely only for small coupling and low temperatures. For quadratic modes, the semiclassical approximation is much more restricted. In Fig. 7(b) the continuous line is the semiclassical line shape. In this figure $\hbar\omega_a=0.0138$, $\hbar\omega_b=0.001$, and $kT=0.04$. Hence, this is an example of a strongly coupled quadratic mode ($\omega_b/\omega_a\ll1$). The semiclassical approximation does not give a good fit to the envelope of the quantum line shape. Thus the semiclassical line shape for quadratic modes will hold only for small frequencies and high temperatures. For tightly bound impurities, the local modes will typically have frequencies on the order of k times the Debye temperature, so that this condition will generally not be satisfied.

The resemblance between the semiclassical line shape, Eq. (4.36), and the Urbach rule for absorption in insulators[23] has led several authors[24,25] to propose that interaction with quadratic modes supplies the low-energy exponential tail of the Urbach rule. As we have seen, it is not possible to obtain a low-energy tail from a quadratic mode at low temperatures. Hence the proposed model for the Urbach rule, although possibly adequate for high temperature, is somewhat suspect

[23] F. Urbach, Phys. Rev. **92**, 1324 (1953).
[24] H. Mahr, Phys. Rev. **132**, 1880 (1963).
[25] Y. Toyozawa, Progr. Theoret. Phys. (Kyoto), Suppl. **12**, 111 (1959). Y. Toyozawa, Institute for Solid State Physics, Tokyo, 1964, Technical Report **A119** (to be published).

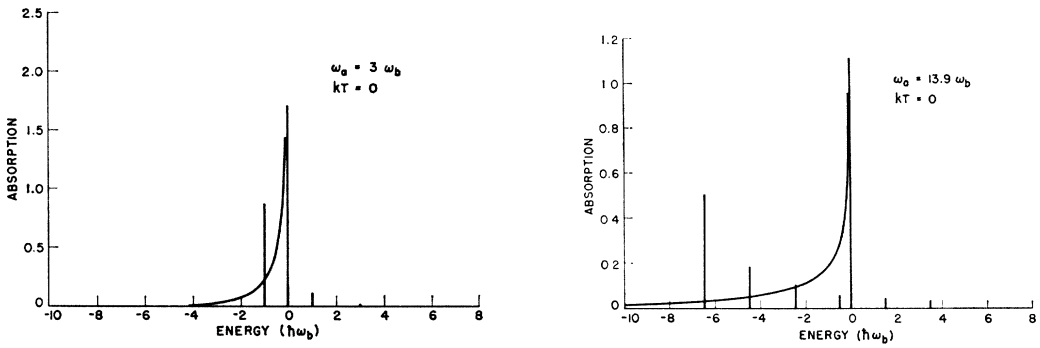

(a) (b)

FIG. 9. Comparison of quantum and semiclassical line shapes for (a) $\omega_a=3\omega_b$ and $kT=0.0$ and (b) $\omega_a=13.9\omega_b$ and $kT=0.0$. The energy variable is $\hbar\omega$ [see Eq. (4.5)], plotted in units of $\hbar\omega_b$.

for temperatures small compared to the relevant frequencies.

Finally, we make a few remarks about the singularity appearing in the semiclassical line shapes, Eqs. (4.36) and (4.37), [and in Eqs. (4.13) and (4.34), the quantum line shapes for $\omega_b\approx 0$]. This singularity is essentially due to a singularity in the Jacobian which takes the probability distribution function for the oscillator from displacement to energy units. The presence of more than one mode removes the singularity, since there is no singularity in the Jacobian for two or higher dimensions. As an example we consider two quadratic modes, where the two ground-state frequencies are ω_a and the two-excited-state frequencies are ω_b, in the semiclassical approximation. The line shape is, for $\omega_b<\omega_a$

$$I_{ab}^{s.c.}(E')=\{\omega_a^2/[kT(\omega_a^2-\omega_b^2)]\}\exp[-(E'/kT)\omega_a^2/(\omega_b^2-\omega_a^2)] \quad (E'<0)$$
$$=0 \quad (E'>0), \tag{4.41}$$

and the singularity is gone. Similarly, for three degenerate quadratic modes, the line shape for $\omega_b<\omega_a$ is

$$I_{ab}^{s.c.}(E')=-2\pi^{-1/2}\{\omega_a^2/[kT(\omega_a^2-\omega_b^2)]\}^{3/2}E'^{1/2}\exp[-(E'/kT)\omega_a^2/(\omega_b^2-\omega_a^2)] \quad (E'<0)$$
$$=0 \quad (E'>0), \tag{4.42}$$

and again no singularity appears. Similar considerations apply to Eqs. (4.13) and (4.34).

V. MANY MODES

We have obtained line-shape functions, for linear modes [Eq. (3.10)] and for quadratic modes [Eq. (4.32)], which consist of a series of evenly spaced δ functions, each multiplied by an appropriate weight factor. Hence in our analysis the most general line-shape function is

$$I_1(E)=\sum_{\gamma=-\infty}^{\infty} P(\gamma)\delta(\gamma\hbar\omega_1+\Delta_1-E). \tag{5.1}$$

Here $P(\gamma)$ is the weight function, $\hbar\omega_1$ is the spacing of the δ functions, and Δ_1 includes the difference in zero-point energy for the ground- and excited-vibrational states.

Consider a second line-shape function due to another mode

$$I_2(E)=\sum_{\beta=-\infty}^{\infty} L(\beta)\delta(\beta\hbar\omega_2+\Delta_2-E), \tag{5.2}$$

where $\hbar\omega_2$ and Δ_2 are, in general, not equal to $\hbar\omega_1$ and Δ_1. The line shape due to both modes is just the convolution of I_1 and I_2. Using one of the δ functions to perform the convolution, we obtain the line-shape function due to both modes

$$I_{12}(E)=\sum_{\gamma=-\infty}^{\infty}\sum_{\beta=-\infty}^{\infty} P(\gamma)L(\beta)$$
$$\times\delta(\gamma\hbar\omega_1+\beta\hbar\omega_2+\Delta_1+\Delta_2-E). \tag{5.3}$$

The arguments of the δ functions in Eq. (5.3) are in a somewhat inconvenient form since they are not arranged in order of increasing energy. To remedy this, we assume there exist integers n_1 and n_2 such that $n_1\omega_1=n_2\omega_2$.

Equation (5.3) becomes

$$I_{12}(E)=\sum_{\gamma=-\infty}^{\infty}\sum_{\beta=-\infty}^{\infty}P(\gamma)L(\beta)\times\delta[(\gamma n_2+\beta n_1)\hbar\omega_2/n_1+\Delta_1+\Delta_2-E]. \quad (5.4)$$

Letting $\alpha=\gamma n_2+\beta n_1$, Eq. (5.4) may be written

$$I_{12}(E)=\sum_{\alpha=-\infty}^{\infty}R(\alpha)\delta(\alpha\hbar\omega_{12}+\Delta_{12}-E), \quad (5.5)$$

where

$$\hbar\omega_{12}=\hbar\omega_2/n_1, \qquad \Delta_{12}=\Delta_1+\Delta_2, \quad (5.6)$$

and the new weight function $R(\alpha)$ is given by

$$R(\alpha)=\sum_{\gamma}{}' P(\gamma)L(\beta), \quad (5.7)$$

where $\sum_\gamma{}'$ means sum over all γ such that $\beta=(\alpha-\gamma n_2)/n_1$ is an integer.

The line-shape function Eq. (5.5) is in the same form as Eqs. (5.1) and (5.2), i.e., a series of evenly spaced δ functions. To include a third mode we simply apply the same method again. In this way all of the N modes assumed to interact are enfolded giving the total line-shape function for the system. Equation (5.5) is easily evaluated by a digital computer. If a smooth line shape is desired, a spectrometer bandpass is included and enfolded with the calculated line shape.

VII. CONCLUSION

We have considered the theory of optical-absorption line shapes for impurities in insulating solids. The theory may also be applied to emission line shapes by simply reversing the role of initial and final states. Within the adiabatic and Condon approximations, and assuming that quadratic cross terms may be neglected or treated by the variational method given here, we have shown that the line shape is given by an N-fold convolution, with each contribution to the convolution being the line shape due to a single normal vibrational mode of the *ground state* of the system. The line shapes due to these modes may be divided into three types, characterized by the difference in the adiabatic potentials of the ground and excited states. The first type is characterized by a term linear in the normal mode displacement. Because of their relative simplicity, only linear modes have been treated in any detail in the past. The second type, characterized by a term quadratic in the normal mode displacement, has received only approximate treatment. We have presented the first thorough quantum treatment of these quadratic modes. Modes of the third type were not treated here. The complexities of quadratic modes are such that the aid of a digital computer is essential for the calculation of line shapes. We have developed computer programs which not only calculate the line shapes but also, using a digital plotter, draw profiles of this line shape.

In addition to the quantum theory of linear and quadratic modes we have also discussed a commonly used approximate method for treating line shapes: the semiclassical approximation. The limitations, range of validity, and relation to the full quantum theory were clearly established. In particular we showed that the semiclassical approximation, although of great value for linear modes, is of limited use for quadratic modes; and in fact often leads to completely erroneous results.

For any realistic impurity system, we expect that a variety of different modes, both linear and quadratic, will interact with the center. Hence, we have developed formal methods for performing the necessary convolutions to obtain the total line shape due to an arbitrary number of interacting modes. These methods will be applied to a model of a simple impurity system, an atomic hydrogen impurity in solid argon, in a forthcoming publication.[26]

Strictly speaking the theory which we have presented applies only to singlet-to-singlet transitions. If the excited state is a member of a degenerate multiplet, the adiabatic approximation is expected to fail, and the theory will not be applicable. These degenerate multiplets have not yet been successfully treated theoretically. The problem of degeneracy must be regarded as one of the major unsolved problems in the theory of absorption line shapes. Experience has shown, however, that many absorption bands involving degenerate multiplets may still be usefully analyzed with the singlet-to-singlet theory. For emission processes the transitions involved are often effectively singlet to singlet and the theory applies directly. The initial state for emission is the *relaxed* excited state and, even though it is still a member of a degenerate multiplet, the different states of the multiplet now differ in their respective lattice configurations. If the vibrational wave functions for these lattice configurations do not overlap appreciably in configuration space (i.e., small dynamical Jahn-Teller coupling), the members of the multiplet are not coupled, and the emission process is effectively singlet to single.

The present theory makes possible and feasible a realistic treatment of the interaction of impurity centers with lattice vibrations. Although assuming interaction with only one linear mode has been successfully used for some centers, we expect that many more types of centers will interact appreciably with a larger number of lattice modes. Hence, it is hoped that the methods developed here will find many applications in the analysis of line shapes for a variety of impurity centers.

---

[26] T. H. Keil and A. Gold (to be published).

ACKNOWLEDGMENTS

The author wishes to express his gratitude to Professor A. Gold for suggesting this problem, and for his aid and advice during the course of the work. Conversations with J. Hernandez are also appreciated.

APPENDIX A

We wish to evaluate the quadratic-mode overlap integral

$$S_{\alpha\beta}=\left(\frac{ab}{\pi 2^{\alpha+\beta}\alpha!\beta!}\right)^{1/2}\int_{-\infty}^{\infty}dq\,\exp[-\tfrac{1}{2}(a^2+b^2)q^2]H_\alpha(aq)H_\beta(bq)\,, \tag{A1}$$

where $a=(m\omega_a/\hbar)^{1/2}$ and $b=(m\omega_b/\hbar)^{1/2}$. We multiply by $t_1{}^\alpha t_2{}^\beta(\alpha!\beta!)^{-1/2}$, sum over α and β, use the generating function for Hermite polynomials[13]

$$\exp(2tz-t^2)=\sum_{n=0}^{\infty}H_n(z)t^n/n!\,, \tag{A2}$$

perform the integral over q, equate equal powers of t_1 and t_2 on the right- and left-hand sides, and obtain for the overlap integral

$$\begin{aligned}
S_{2\alpha,2\beta}&=\left[(1-x^2)^{1/2}\frac{2\alpha!2\beta!}{2^{2\alpha+2\beta}}\right]^{1/2}(-1)^\alpha x^{\alpha+\beta}\sum_{\gamma=0}^{[\alpha,\beta]}\frac{(-1)^\gamma 2^{2\gamma}}{(\alpha-\gamma)!2\gamma!(\beta-\gamma)!}x^{-2\gamma}(1-x^2)^\gamma\,,\\
S_{2\alpha+1,2\beta+1}&=\left[(1-x^2)^{3/2}\frac{(2\alpha+1)!(2\beta+1)!}{2^{2\alpha+2\beta+2}}\right]^{1/2}(-1)^\alpha x^{\alpha+\beta}\sum_{\gamma=0}^{[\alpha,\beta]}\frac{(-1)^\gamma 2^{2\gamma}}{(\alpha-\gamma)!(2\gamma+1)!(\beta-\gamma)!}x^{-2\gamma}(1-x^2)^\gamma\,,
\end{aligned} \tag{A3}$$

where $x=(\omega_b-\omega_a)/(\omega_b+\omega_a)$ and $[\alpha,\beta]$ means the lesser of α and β. Overlaps for which one index is odd, and the other even, vanish because of the parity of the wave functions. The sums over γ may be taken from 0 to ∞, since the denominator of the summand becomes infinite for $\gamma>[\alpha,\beta]$, and cuts off the sum.

The overlaps may be written in terms of hypergeometric functions

$$\begin{aligned}
S_{2\alpha,2\beta}&=\left[(1-x^2)^{1/2}\frac{2\alpha!2\beta!}{2^{2\alpha+2\beta}}\right]^{1/2}(-1)^\alpha x^{\alpha+\beta}(\alpha!\beta!)^{-1}F[-\alpha,-\beta,\tfrac{1}{2};-(1-x^2)/x^2]\,,\\
S_{2\alpha+1,2\beta+1}&=\left[(1-x^2)^{3/2}\frac{(2\alpha+1)!(2\beta+1)!}{2^{2\alpha+2\beta+2}}\right]^{1/2}(-1)^\alpha x^{\alpha+\beta}\Gamma(\tfrac{1}{2})[\alpha!\beta!\Gamma(\tfrac{3}{2})]^{-1}F[-\alpha,-\beta,\tfrac{3}{2};-(1-x^2)/x^2]\,,
\end{aligned} \tag{A4}$$

and in terms of associated Legendre functions

$$S_{\alpha\beta}=(2x)^{-1/2}(1-x^2)^{1/4}(\alpha!\beta!)^{-1/2}(-1)^{\alpha/4-\beta/4-1/4}P_{\alpha/2-\beta/2-1/2}{}^{\alpha/2+\beta/2+1/2}[i(1-x^2)^{1/2}/x]. \tag{A5}$$

Several recurrence relations for $S_{\alpha\beta}$ may be established.

$$\begin{aligned}
(\beta-\alpha)(1-x^2)^{1/2}S_{\alpha\nu}&=x[\beta(\alpha+1)]^{1/2}S_{\alpha+1,\beta-1}+x[\alpha(\beta+1)]^{1/2}S_{\alpha-1,\beta+1}\,,\\
(\beta+1)^{1/2}S_{\alpha,\beta+1}-x\beta^{1/2}S_{\alpha,\beta-1}&=(1-x^2)^{1/2}\alpha^{1/2}S_{\alpha-1,\beta}\,,\\
-x[(\beta+1)(\beta+2)]^{1/2}S_{\alpha\beta}&=x[\alpha(\alpha-1)]^{1/2}S_{\alpha-2,\beta+2}+(\alpha-\beta+2)S_{\alpha,\beta+2}\,,\\
-x[\beta(\beta-1)]^{1/2}S_{\alpha\beta}&=x[(\alpha+1)(\alpha+2)]^{1/2}S_{\alpha+2,\beta-2}+(\alpha-\beta+2)S_{\alpha,\beta-2}\,.
\end{aligned} \tag{A6}$$

The last two of these, together with the phase relations

$$\begin{aligned}
S_{2\alpha,2\beta}&=(-1)^{\alpha+\beta}S_{2\beta,2\alpha}\,,\\
S_{2\alpha+1,2\beta+1}&=(-1)^{\alpha+\beta}S_{2\beta+1,2\alpha+1}\,,
\end{aligned} \tag{A7}$$

and S_{00}, in principle allow one to calculate all of the $S_{\alpha\beta}$.

APPENDIX B

We wish to evaluate the integral in Eq. (4.33). Expanding both brackets in the integrand in powers of $\exp[-\beta_a - i\omega_a t]$, we find

$$I_{ab}(\omega)=\frac{1}{2\pi}\left(\frac{2}{\omega_a}\right)^{1/2}[1-\exp(-\beta_a)]\sum_{m=0}^{\infty}\sum_{l=0}^{\infty}\frac{2m!}{2^{2m}(m!)^2}\frac{2l!}{2^{2l}(l!)^2}\exp[-(l+m)\beta_a]$$
$$\times\int_{-\infty}^{\infty}dt\exp[-i\omega t-i(l+m)\omega_a t]\left(\frac{2}{\omega_a}+it\right)^{l}\left(\frac{2}{\omega_a}-it\right)^{-l-1/2} \tag{B1}$$

The integral in (B1) may be performed[27]

$$\int_{-\infty}^{\infty}dt\exp[-i\omega t-i(l+m)\omega_a t]\left(\frac{2}{\omega_a}+it\right)^{l}\left(\frac{2}{\omega_a}-it\right)^{-l-1/2}$$
$$=-2\pi(4/\omega_a)^{-1/4}[\Gamma(l+\tfrac{1}{2})]^{-1}y^{-3/4}W_{l+1/4,1/4}(4y/\omega_a)\quad(y>0)$$
$$=0\quad(y<0), \tag{B2}$$

where $y=\omega+(l+m)\omega_a$ and $W_{\mu,\nu}$ is the Whittaker function of the second kind.[28] Using the identity[29]

$$W_{\mu+n+1/2,\pm\mu}(x)=(-1)^n n!x^{\mu+1/2}\exp(-x/2)L_n^{2\mu}(x), \tag{B3}$$

where $L_n^m(z)$ is the Laguerre function, the line-shape function may be written

$$I_{ab}(\omega)=(2/\pi^2\omega_a)^{1/2}[1-\exp(-\beta_a)]\sum_{\alpha=0}^{\infty}(\omega+\alpha\omega_a)^{-1/2}\exp(-\alpha\beta_a)\exp[-2(\omega+\alpha\omega_a)/\omega_a]f_\alpha[4(\omega+\alpha\omega_a)/\omega_a], \tag{B4}$$

where

$$f_\alpha(z)=\sum_{m=0}^{\infty}\Gamma(m+\tfrac{1}{2})(m!)^{-1}(-1)^{\alpha-m}L_{\alpha-m}^{-1/2}(z)\quad(z>0)$$
$$=0\quad(z<0). \tag{B5}$$

The $f_\alpha(z)$ are polynomials of the αth degree in z, the first few of which are

$$\begin{aligned}
f_0(z)&=\pi^{1/2},\\
f_1(z)&=\pi^{1/2}z,\\
f_2(z)&=\pi^{1/2}(\tfrac{3}{4}-z+\tfrac{1}{2}z^2),\\
f_3(z)&=\pi^{1/2}(3z/2-z^2+\tfrac{1}{6}z^3),\\
f_4(z)&=\pi^{1/2}(\tfrac{3}{8}-\tfrac{3}{2}z+7z^2/4-\tfrac{1}{4}z^3+z^4/24).
\end{aligned} \tag{B6}$$

---

[27] F. Oberhettinger, *Tabellen Zur Fourier Transformation* (Springer-Verlag, Berlin, 1957), p. 203.

[28] *Bateman Manuscript Project, Higher Transcendental Functions*, edited by H. Erdelyi (McGraw-Hill Publishing Company, Inc. New York, 1953), Vol. I, p. 264.

[29] *Bateman Manuscript Project, Tables of Integral Transforms*, edited by H. Erdelyi (McGraw-Hill Publishing Company, Inc., New York, 1954), Vol. II, p. 432.